

HESPE
Second year meeting

Paulo Simões – University of Glasgow

with Lyndsay Fletcher and Eduard Kontar

Graz, Oct 2-3 2012

Electron rates at loop-top and foot-point sources

Implications for electron acceleration and transport from non-thermal electron rates at loop-top and foot-point sources in solar flares.

Simões, P.J.A. & Kontar, E.P., A&A, 2012, submitted.

4 flares with non-thermal coronal sources

Imaging spectroscopy:

LT: thin-target + thermal

FP: thick-target + thermal

Applied VIS_FWDFIT to scale

CLEAN beam_width

Measured LT source size L in images

$$I_{FP}(\epsilon) = \frac{1}{4\pi R^2} \int_{\epsilon}^{\infty} \dot{N}_{FP} \frac{E_0}{K} \left(\frac{E}{E_0} \right)^{\delta_{FP}-2} Q(\epsilon, E) dE$$

↑
Electron rate at FP (from thick-target)

Results:

NLT/NFP ~ 1.6 (FP fully ionized target, no albedo)

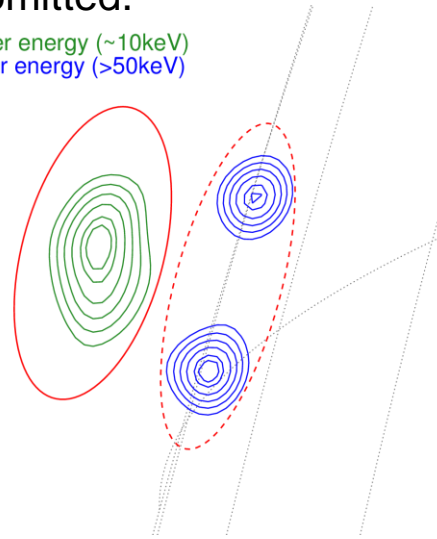
NLT/NFP ~ 8.0 (FP neutral target + albedo)

Implications:

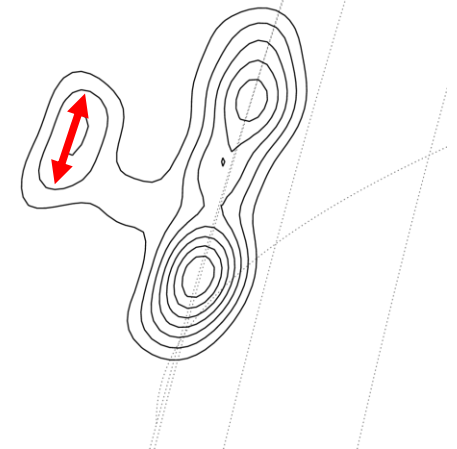
for a beamed injection, trapping alone is not enough, implying pitch-angle scattering;

for an isotropic injection, strong scattering is required in the acceleration process.

lower energy (~10keV)
higher energy (>50keV)



non-thermal coronal source (20~40keV)



$$I_{LT}(\epsilon) = \frac{1}{4\pi R^2} \int_{\epsilon}^{\infty} \langle nV\bar{F}(E) \rangle Q(\epsilon, E) dE$$



$$\dot{N}_{LT} = \left(\frac{DA}{EM} \right)^{1/2} \frac{\langle nV\bar{F}_0 \rangle}{L}$$

↑
Electron rate at LT (from thin-target)

Non-thermal coronal sources

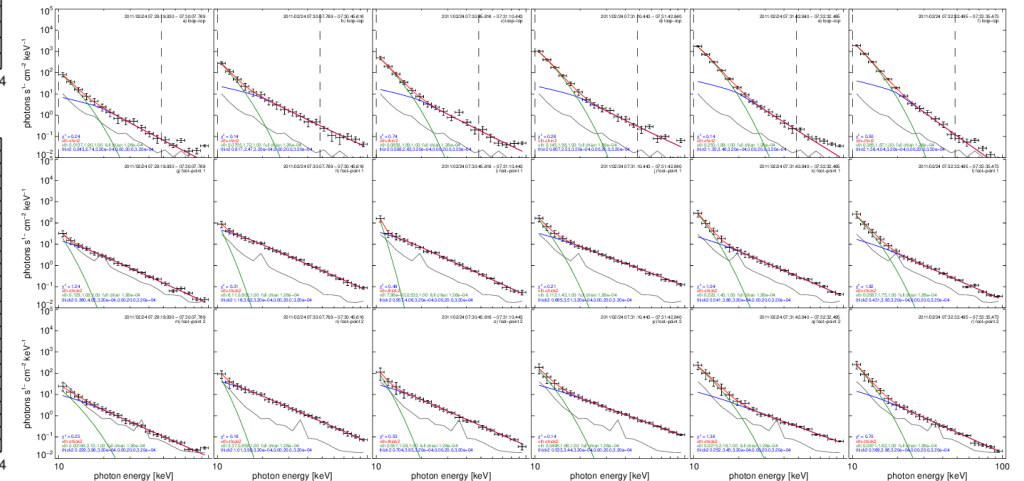
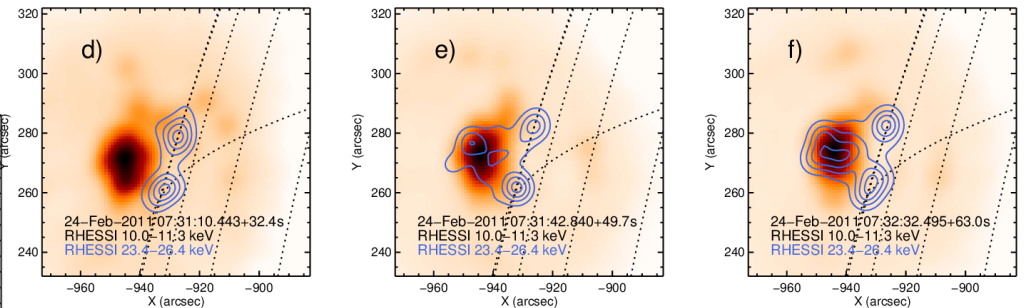
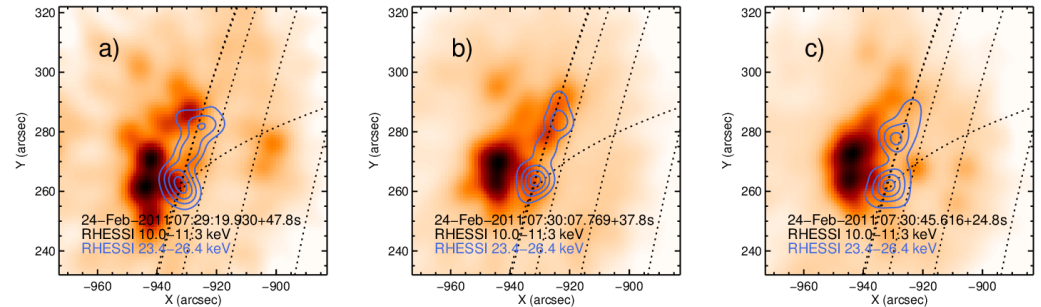
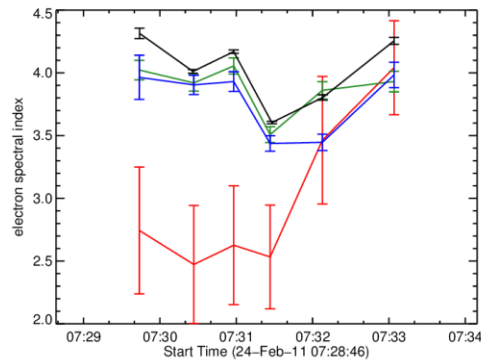
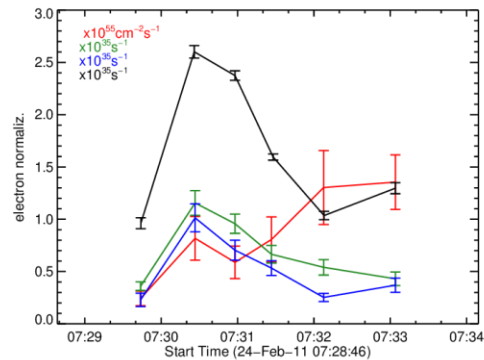
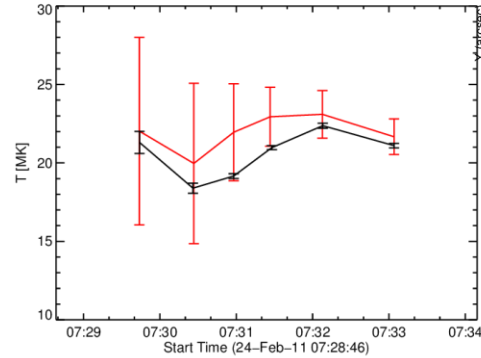
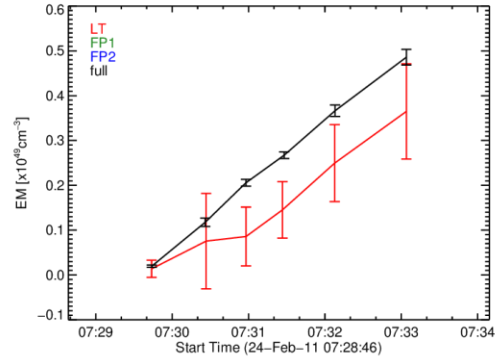
Simões, P.J.A. & Kontar, E.P.

Imaging spectroscopy during rise, peak, decay phases of flares

In 4 flares: resolved coronal source appears after the main peak or decay phase

more efficient thin-target:

- increase of EM
- electron flux at FP is decreasing

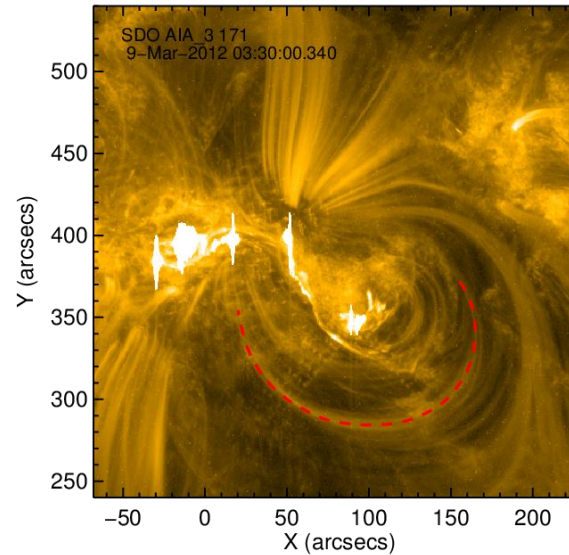
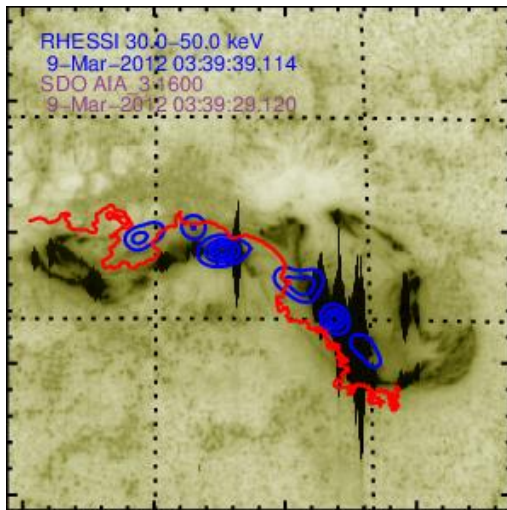


HXR from sheared two-ribbon flare

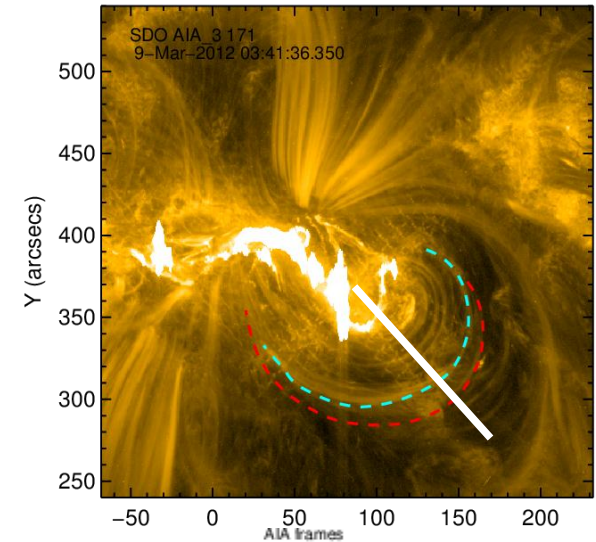
Simões, P.J.A., Fletcher, L. and Hudson, H.

2012 March 09 ~03:40UT M6.4 class

RHESSI foot-points (30-50keV)
along AIA ribbons



171 Å loops collapsing
during HXR impulsive phase

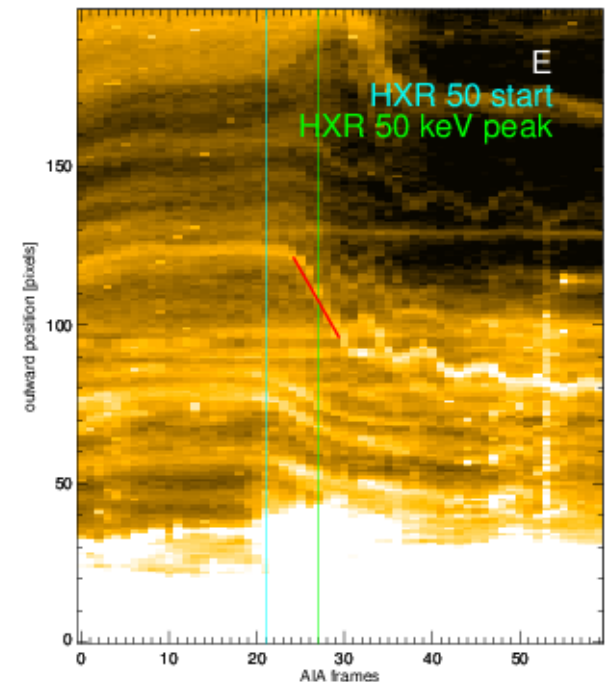


94 Å arcades connecting the ribbons and HXR foot-points
Co-spatial HXR and microwave emission (NoRH 17-34 GHz)

Investigating:

Loops imploding and oscillating: anything in HXR or MW emission?

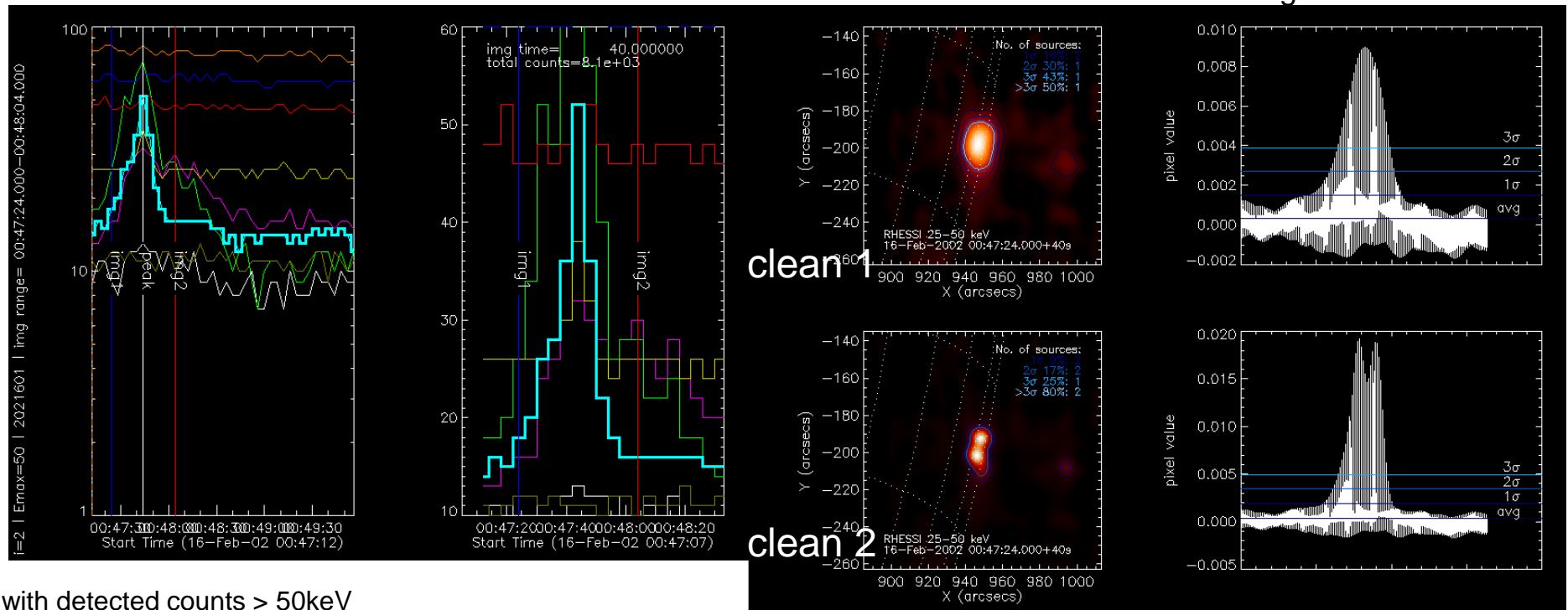
Expansion and dimming of outer loops: CME launch?



HXR Flare Morphology (task 3)

Simões, P.J.A. & Fletcher, L.

Count the number of sources
above 3-sigma level

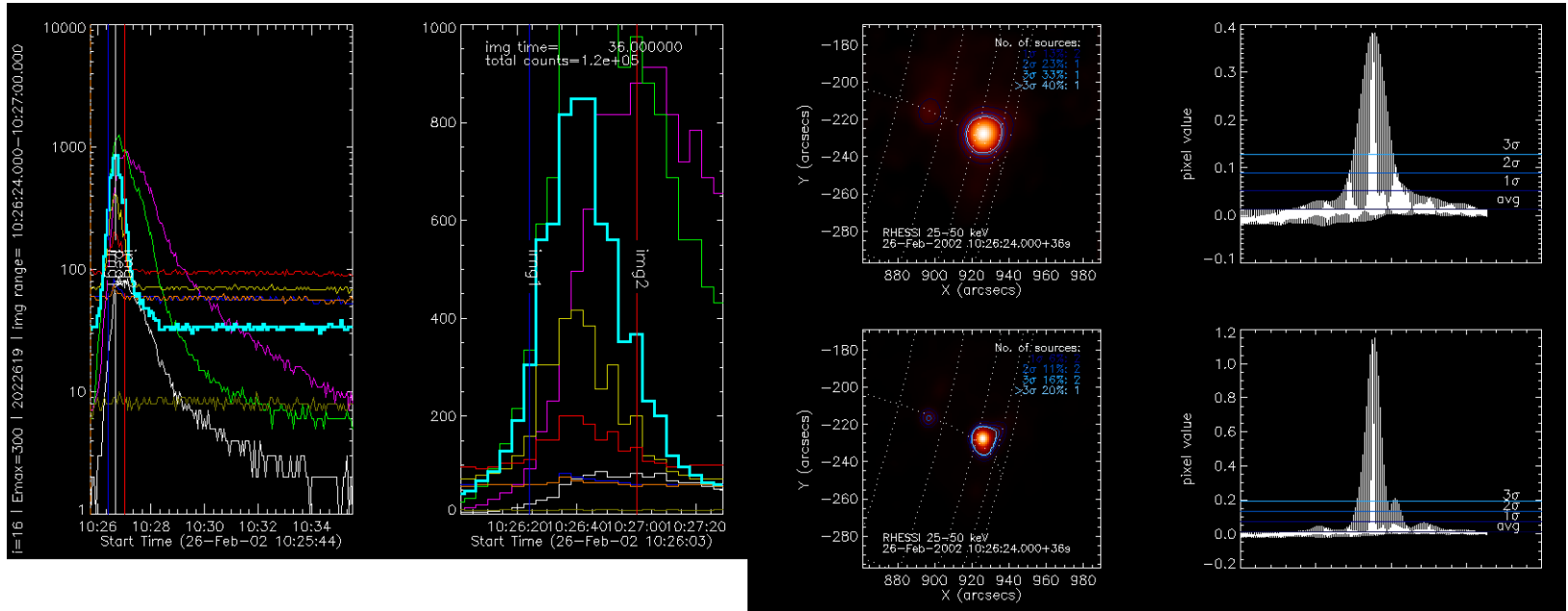


Flare with detected counts > 50keV
~1200 flares (`hsi_read_flarelist()`)
CLEAN images:
beam_width 1 and 2
Peak time of 25-50 keV (≤ 40 secs)
+ 9-12 keV
+ 25-50 keV

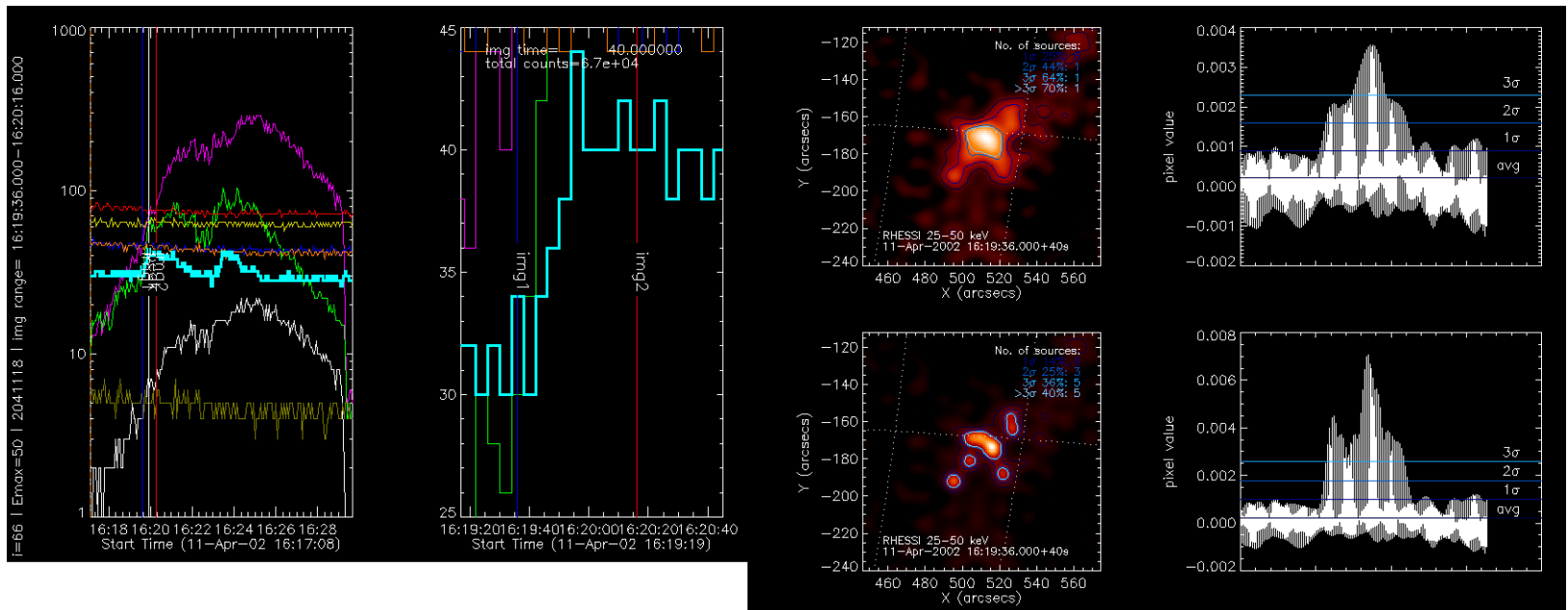
Improving:
+ script for CLEAN images (position)
+ script `vis_fwdfit` to scale beam_width
+ automatic counting
+ using other data to identify true sources (AIA ribbons)

	Number of sources			
beam_width	no image / noise	1	2	>2
1	15.0%	64.3%	19.9%	0.8%
2	9.3%	24.5%	35.2%	31.1%*

Unresolved source



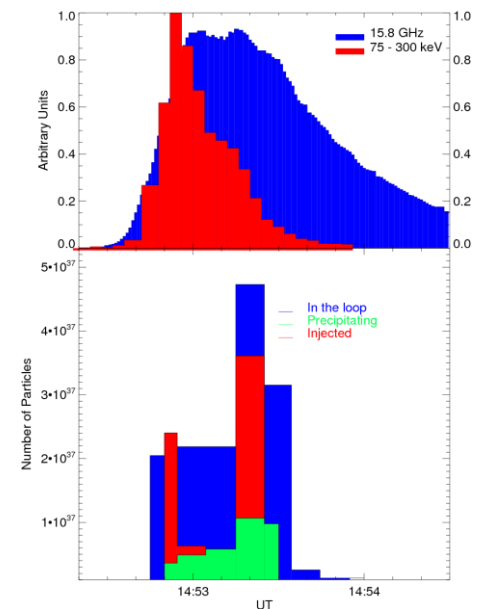
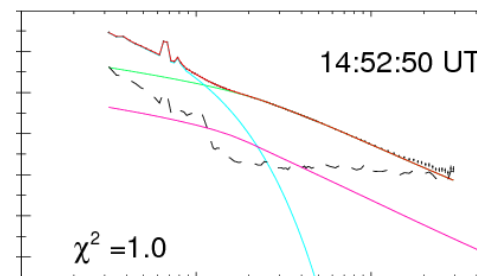
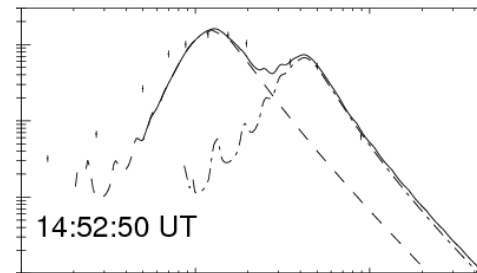
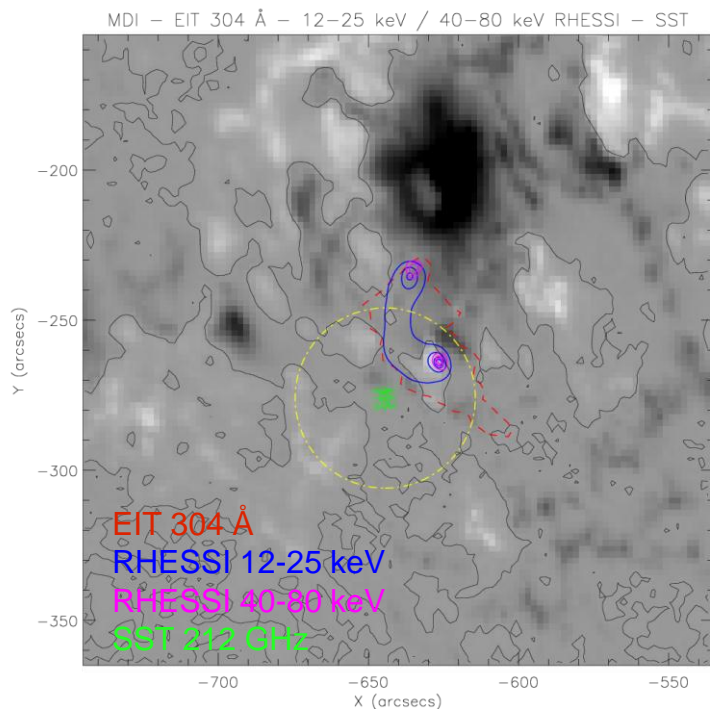
Over-resolved source? (clean 2): other data to identify true sources (AIA 1600 ribbons)



A burst with double radio spectrum observed up to 212 GHz

Giménez de Castro, Cristiani, **Simões**, Mandrini, Correia, Kaufmann, Sol. Phys., 2012, accepted.
HESPE support acknowledged

Flare with double radio spectrum M2.9 10 Sep 2002



After spectral analysis:
two electron populations or broken power-law
+ mildly relativistic (HXR and MW1)
 Loop geometry (HXR)
+ relativistic (MW2)
 Co-spatial or 2nd loop (inferred from MDI analysis)
 SST (212GHz) centroids

Spectral + time analysis:
Evolution of number of electrons
- injected
- trapped
- precipitating